Supporting Information

Mitochondria-localized dinuclear iridium(III) complexes for two-photon photodynamic therapy

Zanru Tan,[a] Jiang Feng,[b] Jiangping Liu,*[c] Taihong Liu,*[b] Huihui Wu,*[d] and Hui Chao*[a]

[a] *MOE Key Laboratory of Bioinorganic and Synthetic Chemistry, Guangdong Basic Research Center of Excellence for Functional Molecular Engineering, School of Chemistry, Sun Yat-Sen University, Guangzhou, 510275, P. R. China. Email: ceschh@mail.sysu.edu.cn*

[b] *Key Laboratory of Applied Surface and Colloid Chemistry of Ministry of Education, School of Chemistry and Chemical Engineering, Shaanxi Normal University, Xi'an, Shaanxi 710119, P. R. China. E-mail: liuth121@snnu.edu.cn*

[c] *The Institute of Flexible Electronics (IFE, Future Technologies), Xiamen University, Xiamen, 361102, P. R. China. Email: liujping@xmu.edu.cn*

[d] *Department of Dermatology, The East Division of the First Affiliated Hospital, Sun Yat-Sen University, Guangzhou, 510700, P. R. China. E-mail: cometvivi@126.com*

Table of Contents

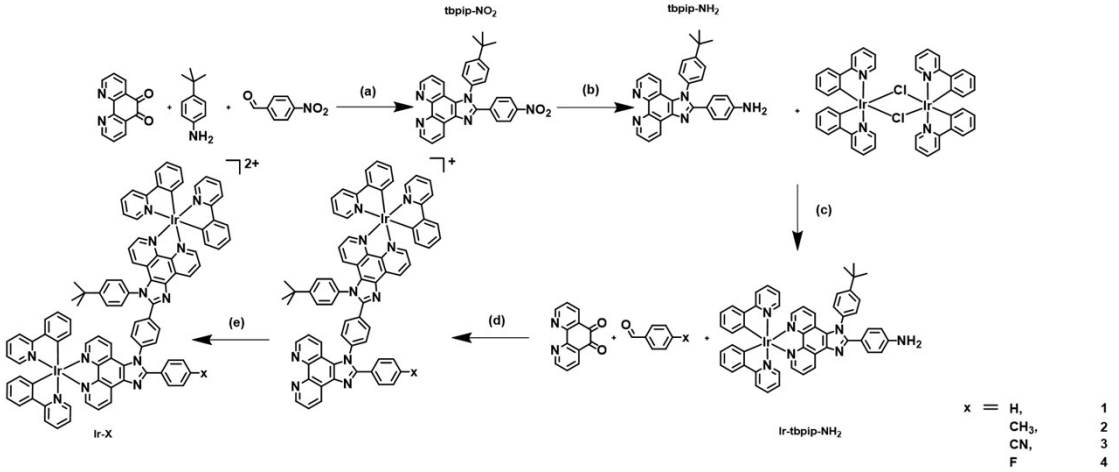

Fig. S1 Synthetic route of the **Ir(III)** complexes. (a) NH_4OAc, HOAc, 120 °C, 12 h; (b) Pd/C, EtOH, H_2O_2, 65°C, 12 h; (c) DCM/MeOH(1:1, v/v), Ar, 85 °C, 6 h; (d) NH_4OAc, HOAc, 135 °C, 12 h; (e) DCM/MeOH(1:1, v/v), Ar, 85 °C, 6 h.

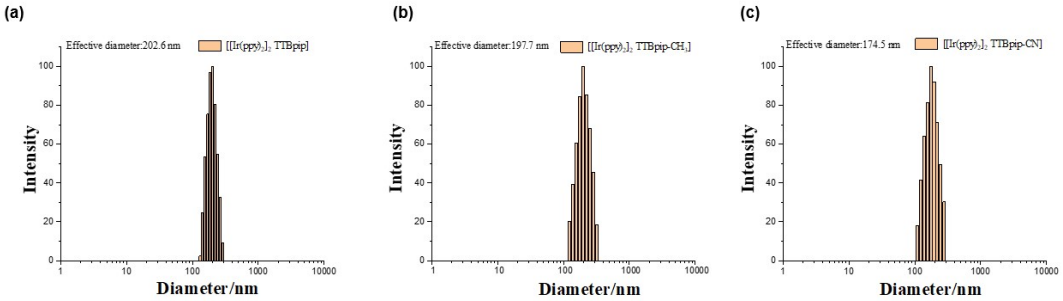

Fig. S2 Size distribution of (a) **N-Ir1**, (b) **N-Ir2,** (c) **N-Ir3** determined by dynamic light scattering.

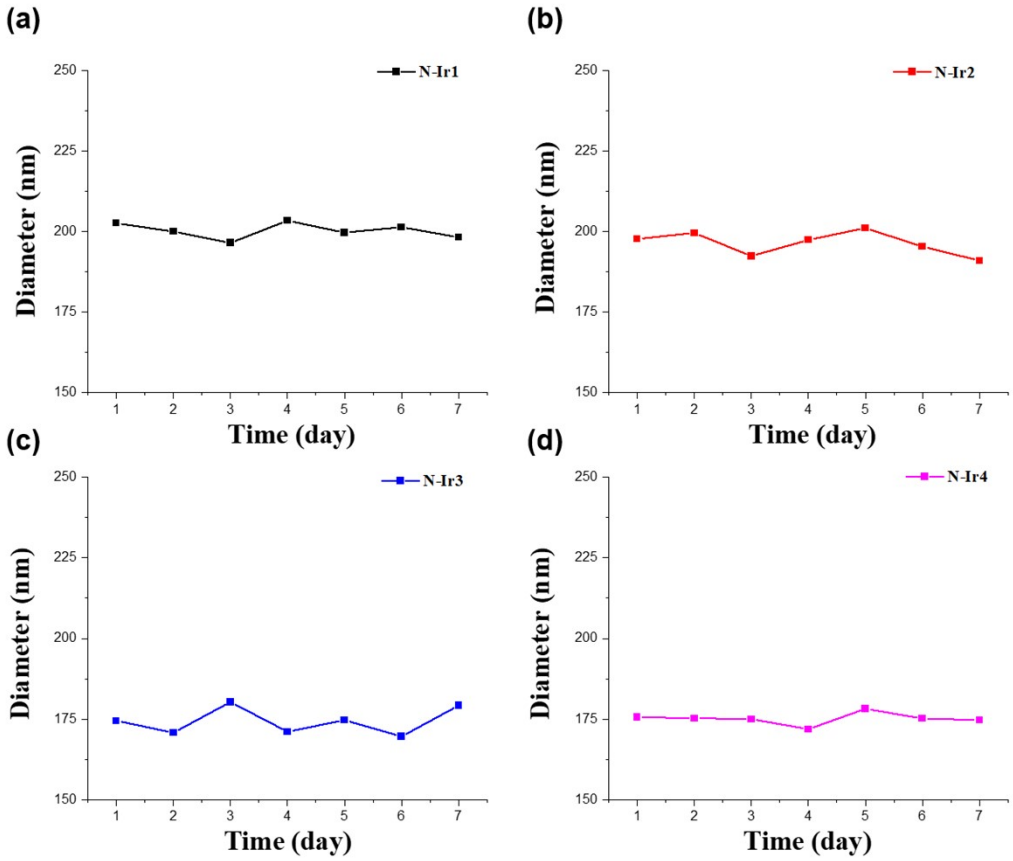

Fig. S3 Long-term stability evaluation for different nanoparticles. (a) **N-Ir1**, (b) **N-Ir2**, (c) **N-Ir3**, (d) **N-Ir4**.

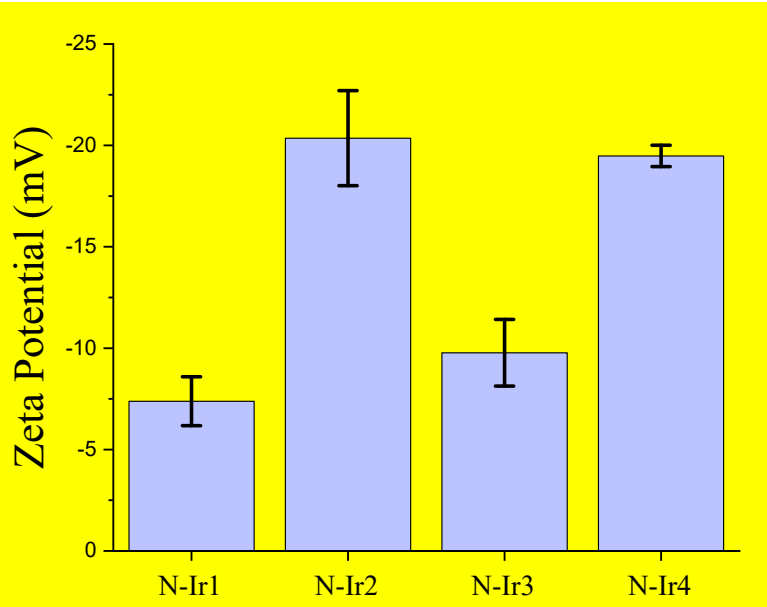

Fig. S4 Zeta potentials of N-Ir1-4 in physiological pH aqueous solution.

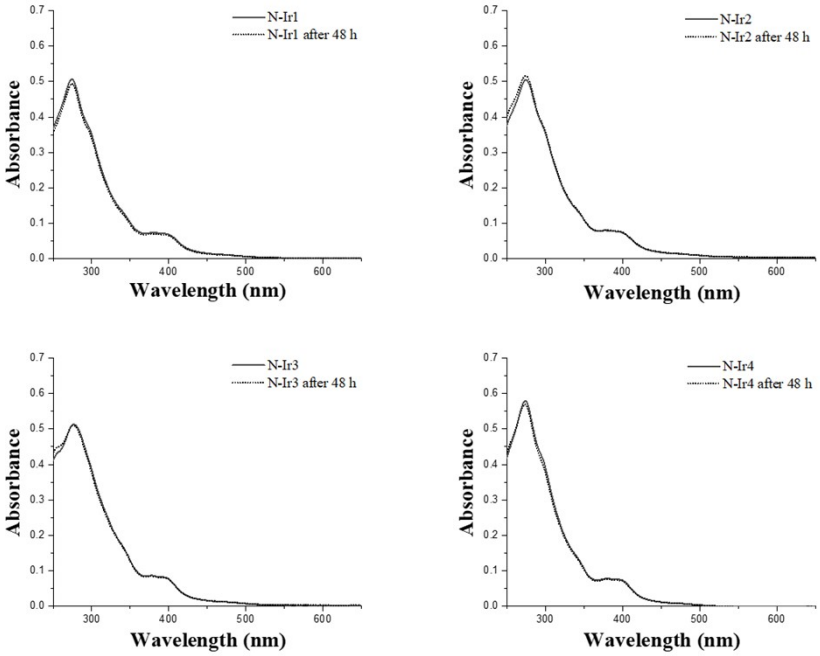

Fig. S5 UV–Vis spectra of the N-Ir1-4 in PBS for 48 h.

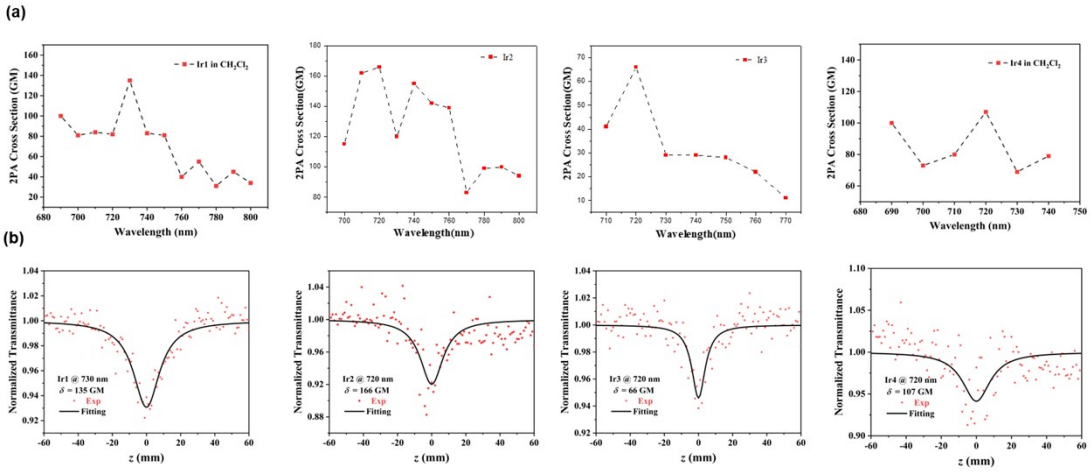

Fig. S6 (a) Two-photon absorption cross section of **Ir1-4** in dichloromethane (c ~ 1.0 $\times 10^{-2}$ M). (b) OA Z-scan data of **Ir1-4**. Open scattered symbols represent experimental data and solid lines are fits resulting from 2PA, The solid lines represent the fits for 2PA.

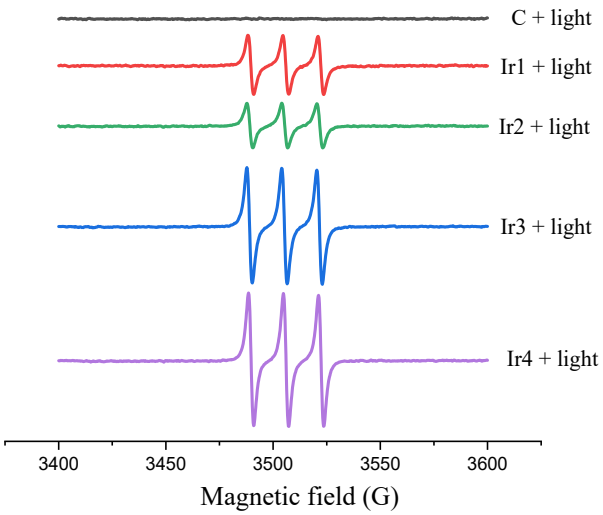

Fig. S7 ESR spectra of **Ir1-4** in the presence of TEMP.

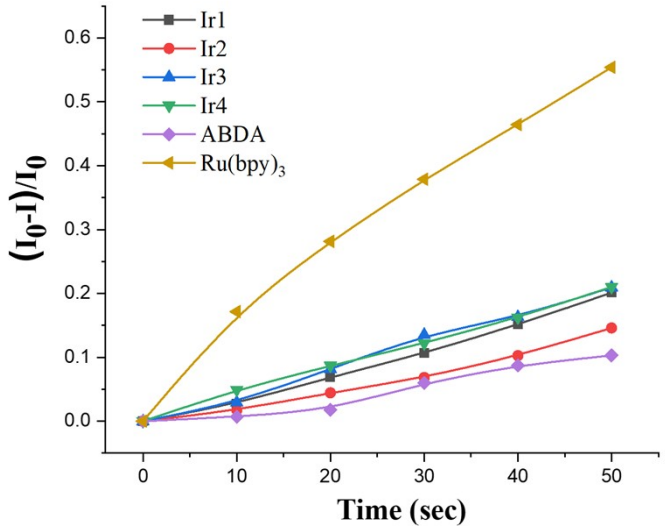

Fig. S8 Plots of the cumulative decrease in optical density of ABDA (100 μM) at 378 nm along irradiation time (λ_{irr}=405 nm) in the presence of the indicated complexes. $[Ru(bpy)_3]^{2+}$ as the standard.

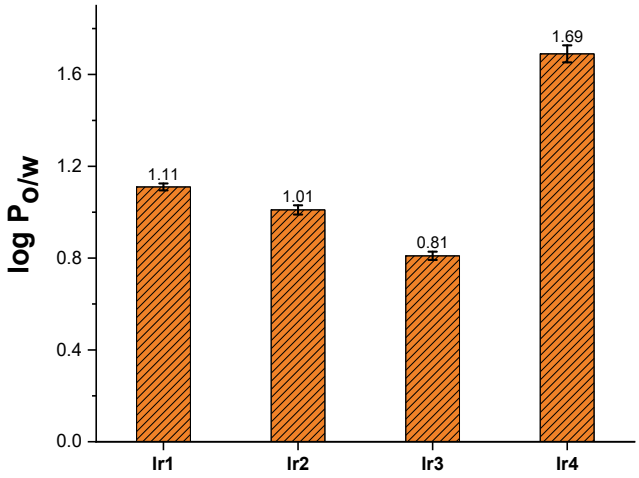

Fig. S9 Partition coefficient (log Po/w) of the indicated complexes. All the experiments were performed as duplicates of triplicates (n = 3 independent experiments). The error bars represent the standard deviation (SD).

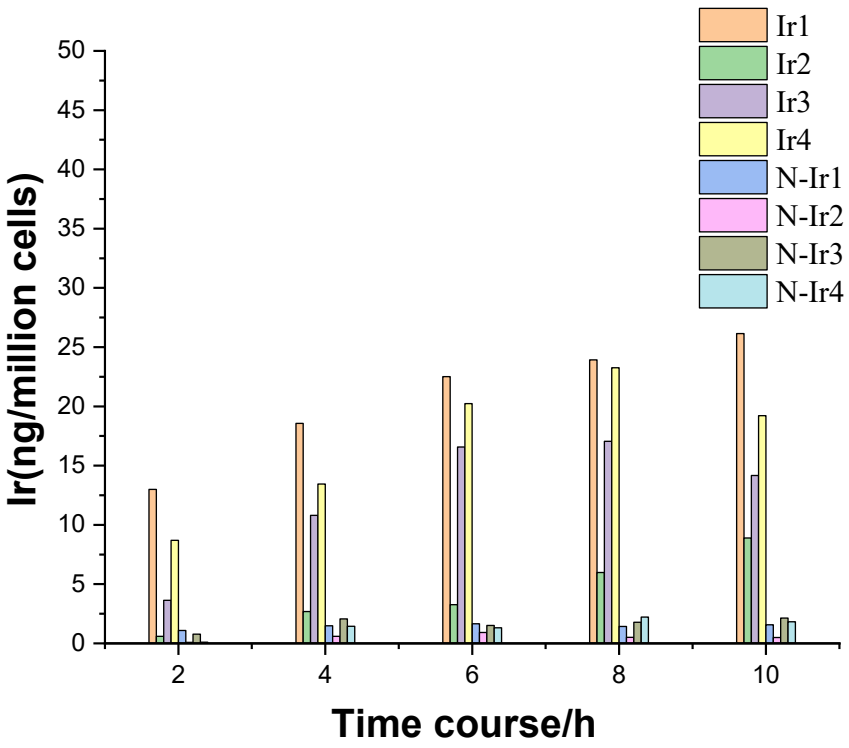

Fig. S10 Time-dependent ICP-MS of A375 cells pre-incubated with **Ir1-4** and **N-Ir1-4** (4 μM).

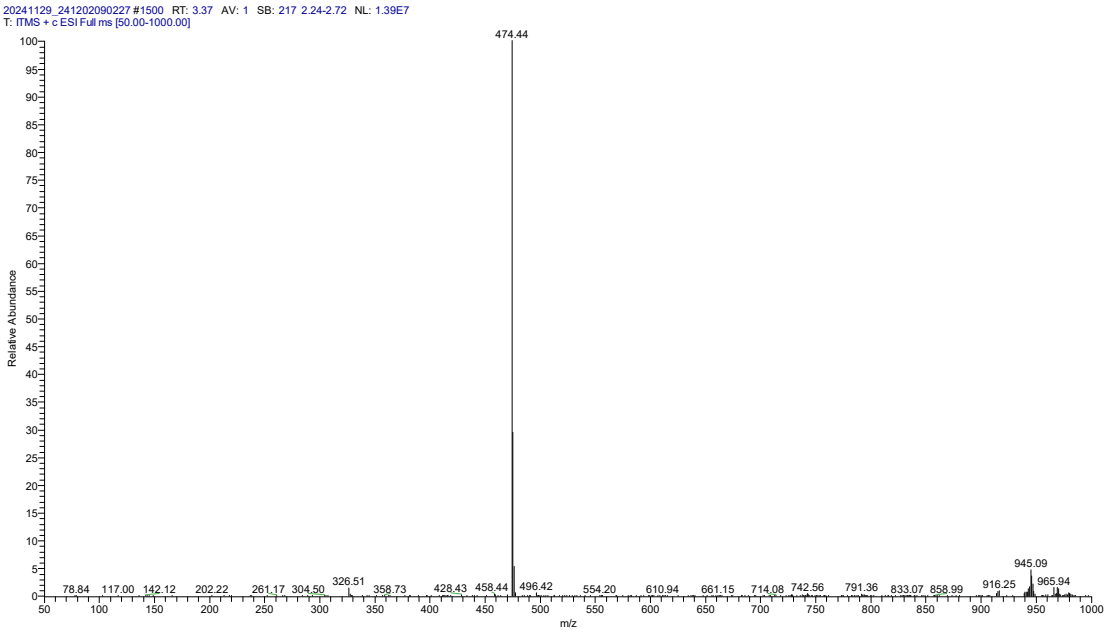

Fig. S11 MS spectrum of the ligand tbpip-NO_2

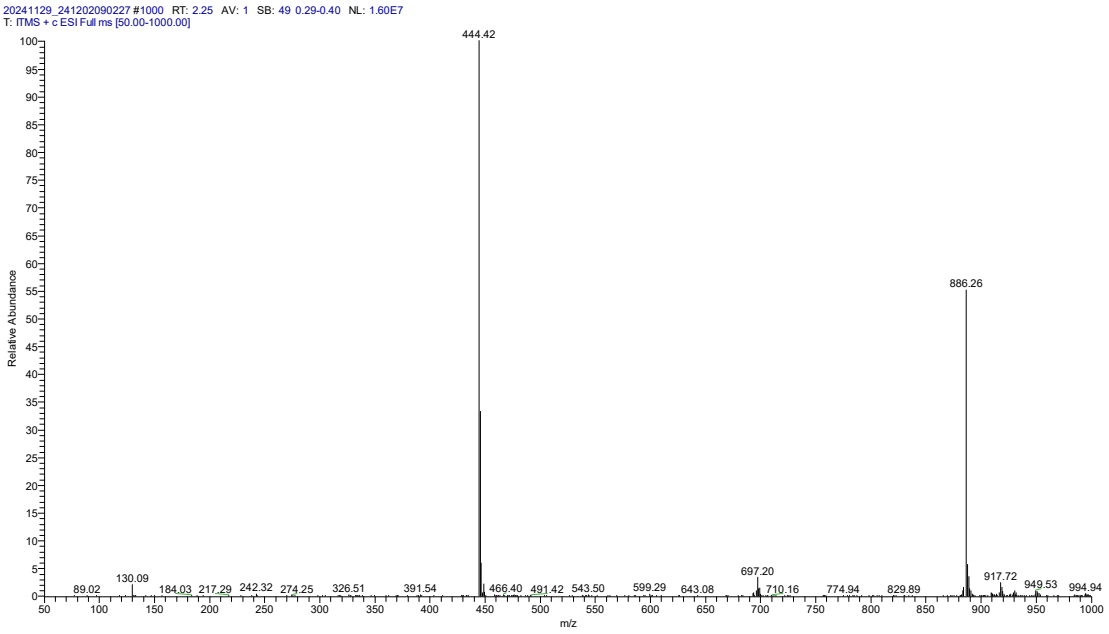

Fig. S12 MS spectrum of the ligand tbpip-NH_2

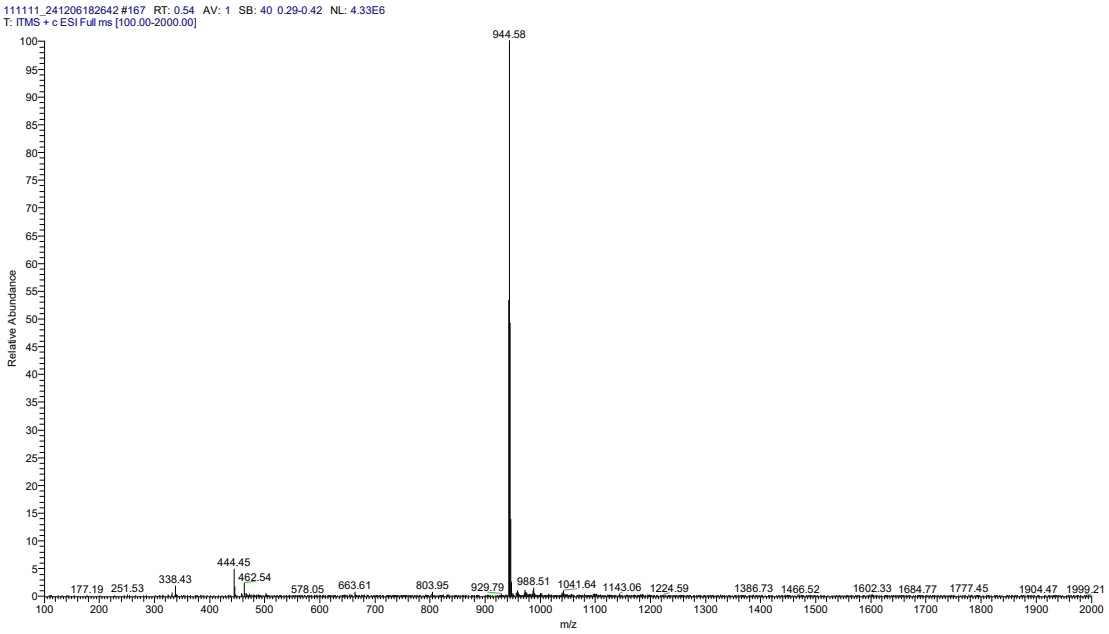

Fig. S13 MS spectrum of **Ir-tbpip-NH_2**

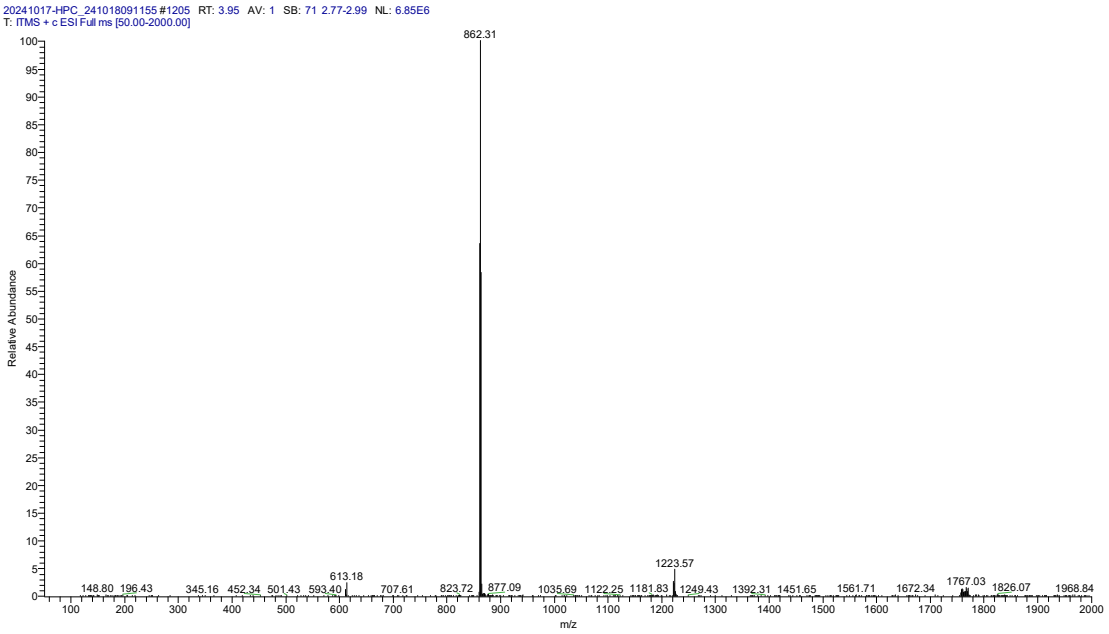

Fig. S14 MS spectrum of **Ir1**

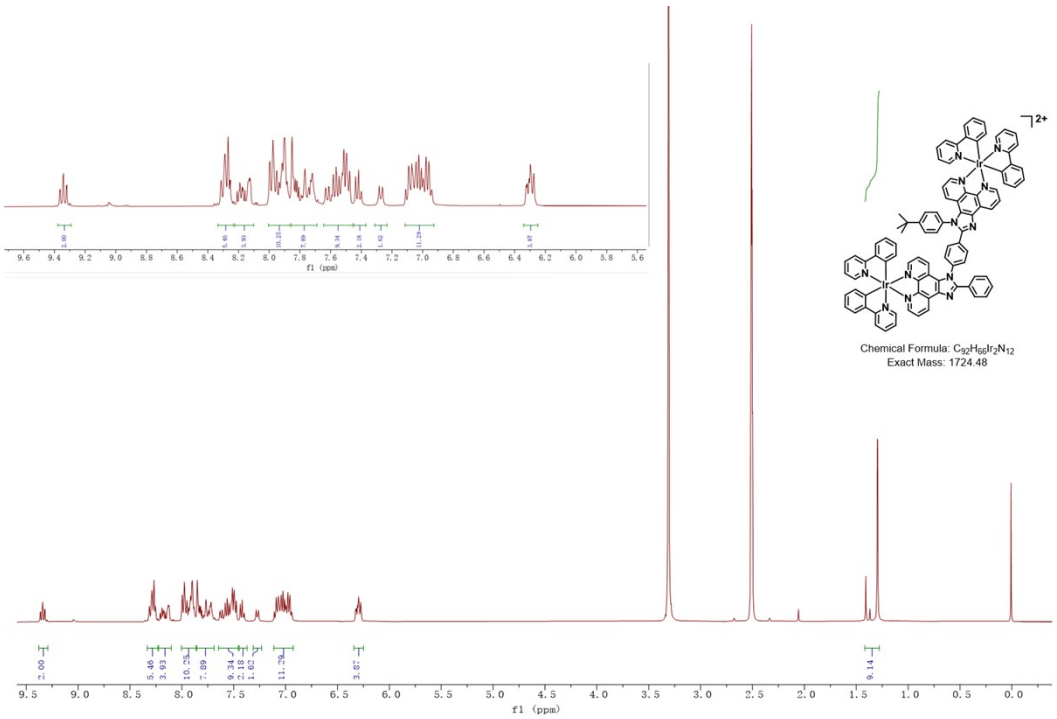

Fig. S15 ^{1}H NMR spectrum of Ir1

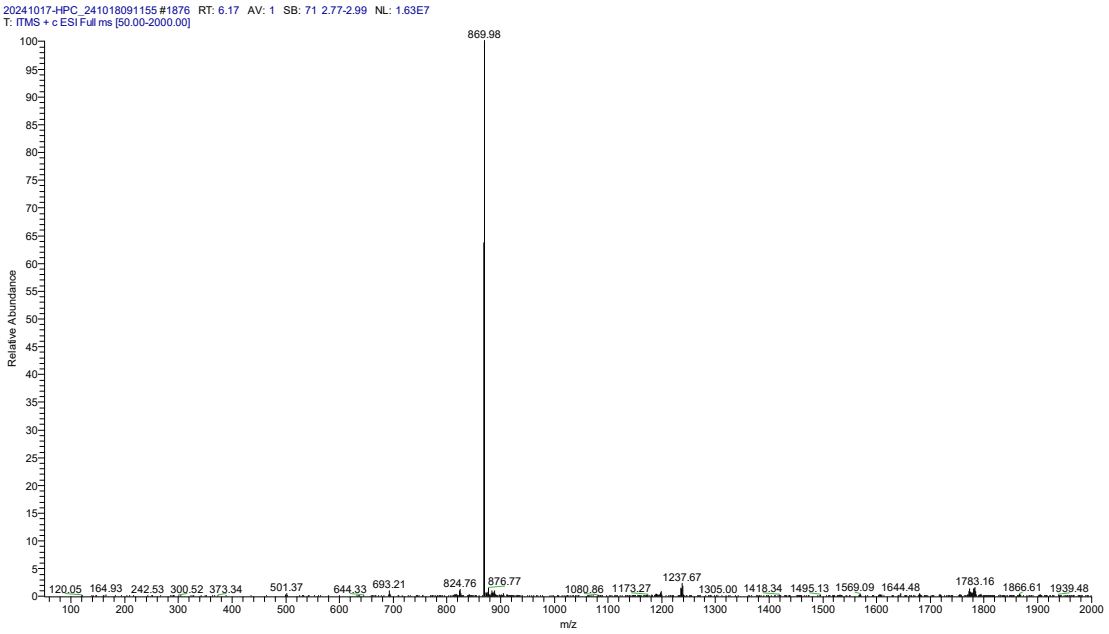

Fig. S16 MS spectrum of **Ir2**

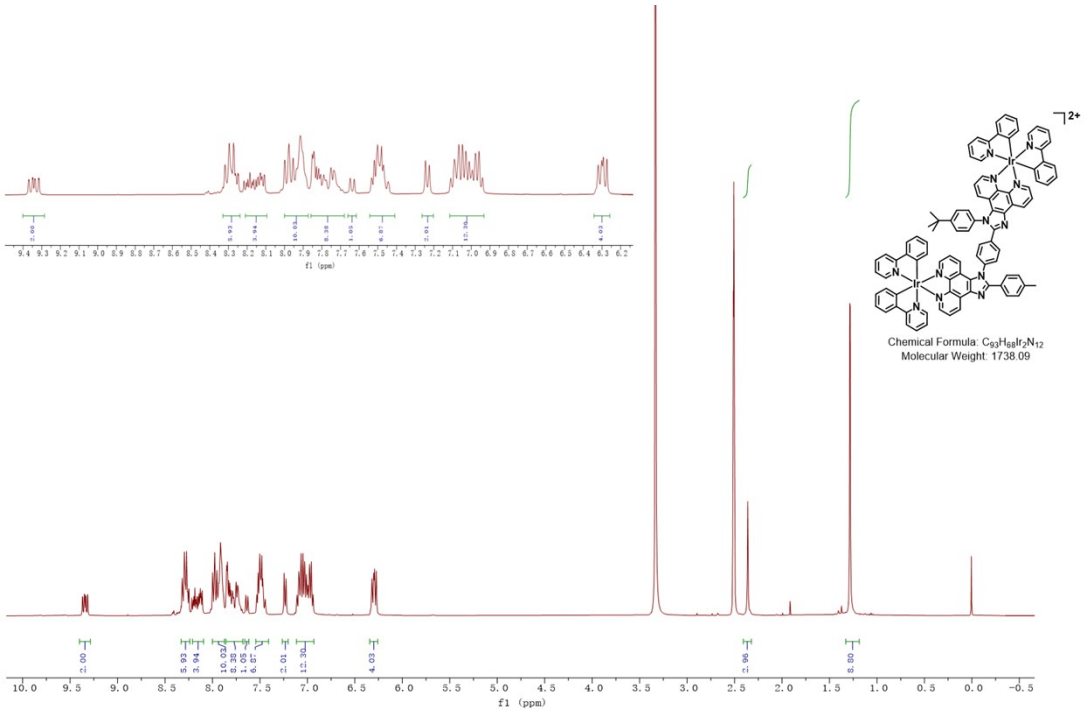

Fig. S17 ^{1}H NMR spectrum of Ir2

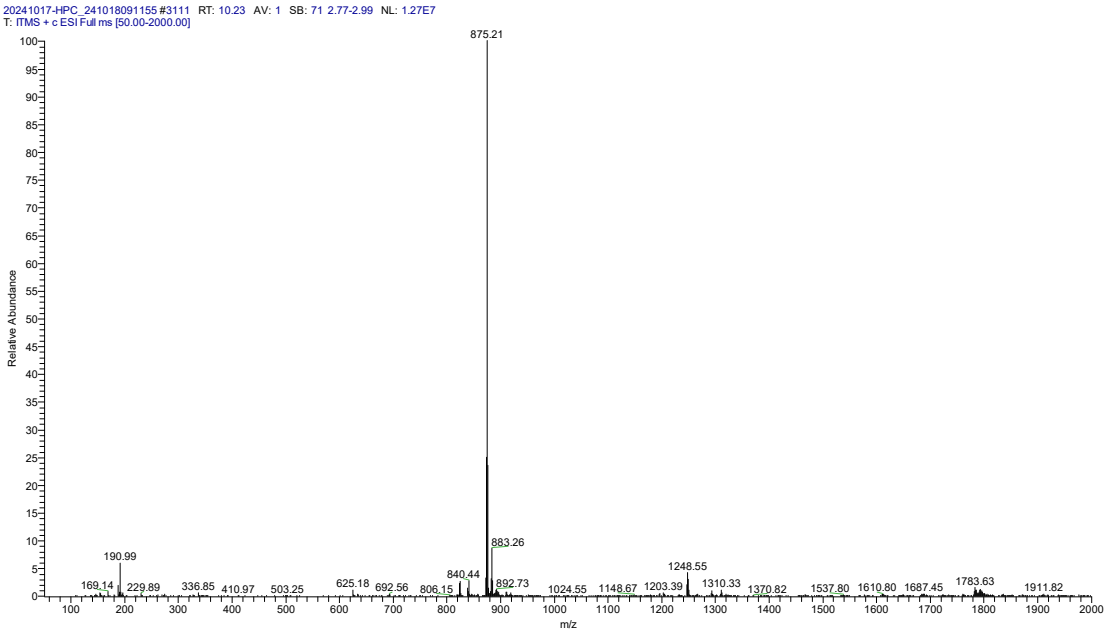

Fig. S18 MS spectrum of **Ir3**

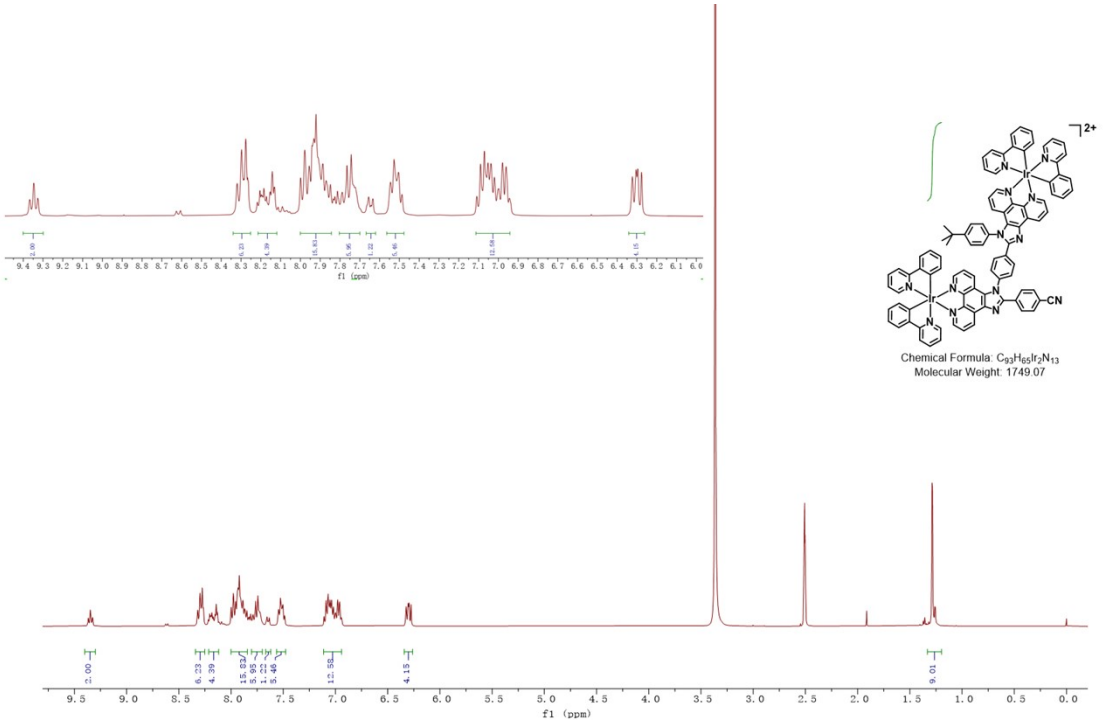

Fig. S19 ^{1}H NMR spectrum of Ir3

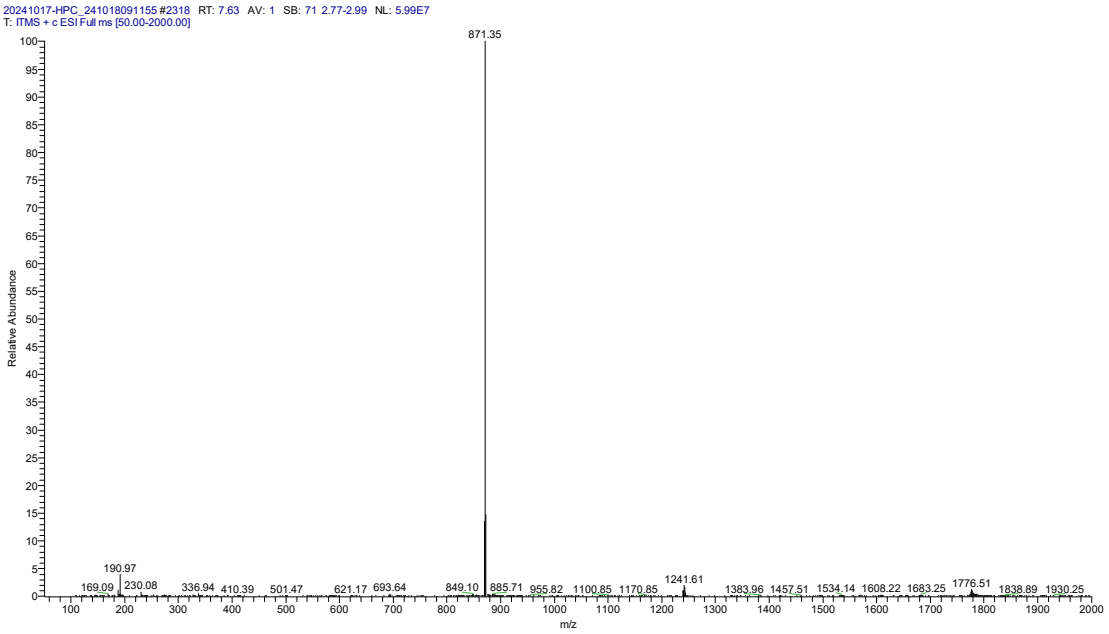

Fig. S20 MS spectrum of **Ir4**

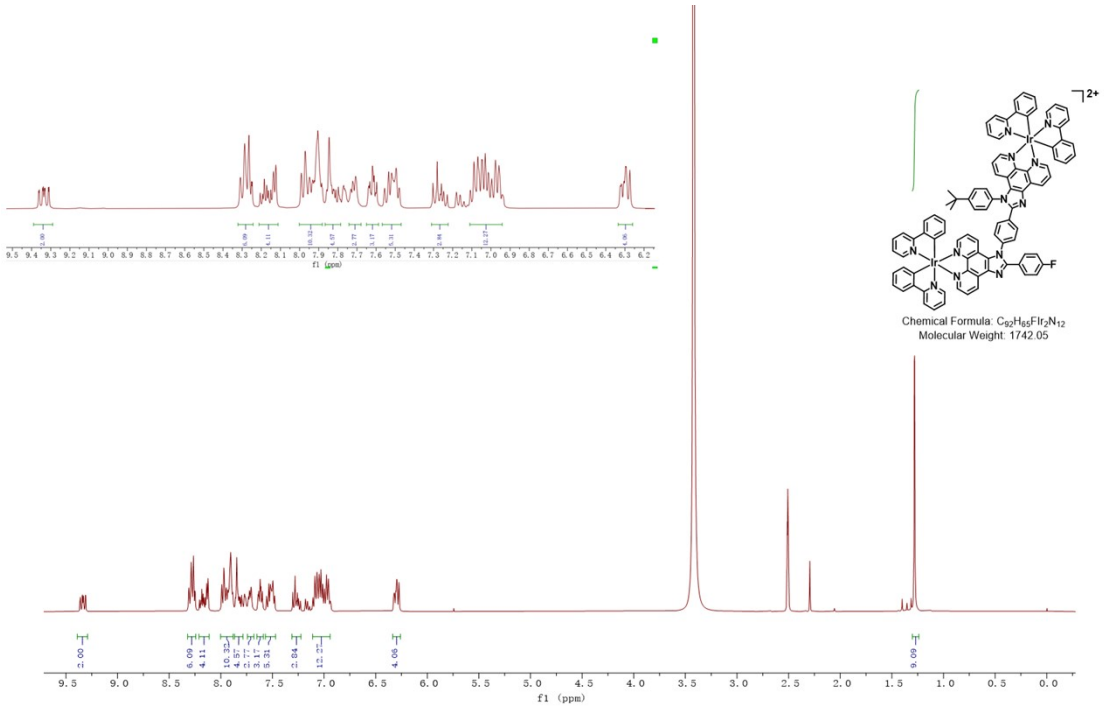

Fig. S21 ^{1}H NMR spectrum of Ir4

Table S1 Photophysical properties of designed compounds

Compd	λ_{abs}/nm (ε, × 10^3 $M^{-1}\cdot cm^{-1}$)	$\lambda_{em/nm}$	Φ_u(air)	τ/ns
Ir1	275, 385, 404	568	0.0198	203
Ir2	274, 385, 404	569	0.0182	201
Ir3	275, 383, 401	570	0.0187	201
Ir4	273, 385, 403	570	0.0193	200

Wavelength/nm	690	700	710	720	730	740	750	760	770	780	790	800
Ir1 δ_{2PA}/GM	100	81	84	82	135	83	81	40	55	31	45	34
Ir2 δ_{2PA}/GM	--	115	162	166	120	155	142	139	83	99	100	94
Ir3 δ_{2PA}/GM	--	--	41	66	29	29	28	22	11	--	--	--
Ir4 δ_{2PA}/GM	100	73	80	107	69	79	--	--	--	--	--	--

Table S2. 2PA cross sections of Ir1-4 with different excitation wavelengths.

Table S3 Single oxygen quantumn yields of complexes.

Compd	$Ru(bpy)_3^{2+}$	**Ir1**	**Ir2**	**Ir3**	**Ir4**
Φ_Δ	0.81	0.31	0.22	0.32	0.31